

Projective Clustering Product Quantization

Aditya Krishnan
Pinecone, Johns Hopkins University
akrish23@jhu.edu

Edo Liberty
Pinecone
edo@pinecone.io

Abstract

This paper suggests the use of projective clustering based product quantization for improving nearest neighbor and max-inner-product vector search (MIPS) algorithms. We provide anisotropic and quantized variants of projective clustering which outperform previous clustering methods used for this problem such as ScaNN. We show that even with comparable running time complexity, in terms of lookup-multiply-adds, projective clustering produces more quantization centers resulting in more accurate dot-product estimates. We provide thorough experimentation to support our claims.

1 Introduction

In vector similarity search one preprocesses n vectors $x \in \mathbb{R}^d$ such that, given a query $q \in \mathbb{R}^d$ computing the top (or bottom) k values of $f(x, q)$ is most efficient. The function f can encode similarity between x and q like dot product $\langle x, q \rangle$, cosine similarity $\langle x, q \rangle / \|x\| \|q\|$ or Jaccard Similarity. In these cases high values of f are sought. Alternatively, f can encode dissimilarity or distance in which case, low values are searched for. Examples include $f(x, q) = \|x - q\|_p = (\sum_i (x_i - q_i)^p)^{1/p}$, or hamming distance. The reader should be aware that all the above problems are highly related and solutions for one often translate to solutions for another. For example, max cosine similarity, max dot product and min Euclidean distance are all equivalent for unit vectors.

In recent years, vector similarity search has taken center stage in the deployment of large scale machine learning applications. These include duplicate detection [40, 41, 46], personalization [16, 39], extreme classification [9], and more. The demand for vector search was further fueled by proliferation of pre-trained deep learning models which provide semantically rich vector embeddings for text, images, audio, and more [7, 42, 43]. The scale of these problems often requires searching through billions of vectors or performing thousands of searches a second. Performance is therefore paramount which necessitates the use of approximate algorithms. These algorithms trade some tolerance for inaccuracy in the result set with speed. Practical considerations also need to consider indexing speed, index size, concurrent read-write support, support for inserts and deletes, and many other factors. The exact tradeoffs between these factors are both complex and data dependent. Due to the importance and complexity of this task, significant academic and industrial efforts were invested in approximate vector search algorithms [6, 22, 25].

Algorithms fall generally into a handful of categories. Hashing based algorithms [3, 35, 36], tree-search based algorithms [8, 28] and graph based algorithms [19, 25] mostly focus on reducing the dependence on n , the number of vectors. Dimension reduction [5, 24, 38] and quantization

	Centers	Application Time	Index Size
Clustering	k	$kd + n$	$n \log_2(k)$
Product Quantization (PQ)	k^m	$kd + 2nm$	$nm \log_2(k)$
Product Quantization (PQ) with ks centers (for comparison)	$(ks)^m$	$skd + 2nm$	$nm \log_2(ks)$
Quantized Projective Clustering (Q-PCPQ)	$(ks)^m$	$kd + skm + 2nm$	$nm \log_2(ks)$

Table 1: Number of centers, application time to compute inner-products of all points with a query and index size (in bits) for: vanilla clustering, clustering with product quantization, and quantized projective clustering.

algorithms [14, 15, 17, 18, 26, 27, 30, 44, 45], on the other hand, reduce the dependence on d by compressing the index vectors and computing similarities to these compressed representations quickly. To achieve the best results for a specific application, usually a combination of the above methods is needed. Versatile libraries like Faiss [22] along with managed cloud services like Pinecone [1] make these a lot easier for scientists and engineers to use in production applications.

In this paper we focus solely on quantization techniques for approximate max inner product search (MIPS). Simple quantization can be achieved with clustering, specifically, a small representative set of k vectors is chosen and each vector in the data is projected onto that set. Computing the dot products of the query and centers requires only $O(dk)$ time. Then, computing the approximate dot product for each point can be done in $O(1)$ time by a simple lookup. The shortcoming of this approach is that the quantization is very coarse; it allows for only k possible quantization centers. More advanced product quantization techniques divide the d coordinates to m contiguous sections and project each set of d/m coordinates onto one of k centers independently. The advantage of this is that computing the dot product of the query and the centers still requires $O(dk)$ operations but now each point can map to one of k^m centers. The price of this approach is that computing the approximate dot product requires m lookups and additions instead of a single lookup. Clearly, increasing the values of m and k improves the quality of the approximation while also increasing search running time.

In order to improve the tradeoff between increasing running time and increasing the number of cluster centers, we propose projective clustering product quantization (PCPQ). The motivation is to significantly increase the number of cluster centers (and thereby improve vector approximation) while, at the same time, having negligible increase in application running time. The exact definition of projective clustering is given in Section 2. Unlike standard clustering, each data point is projected to a point along the direction of the center c . Specifically, point i projects to $\alpha_i c_j$ where c_j is one of k “centers” in \mathbb{R}^d and $\alpha_i \in \mathbb{R}$ is a scalar. Since α_i is chosen for each point separately, the solution is strictly more general than clustering. Our experimental results below corroborate that this indeed provides a significant increase in approximation quality. Unfortunately, it also requires storing an extra floating point for each point and section of coordinates. This is both inefficient in terms of memory consumption and slow in application time since each lookup-add in PQ is replaced with a lookup-multiply-add in PCPQ.

To address this, we suggest a quantized version of PCPQ (Q-PCPQ). In Q-PCPQ each α_i is chosen from a set of at most s values. As a result, using a lookup table of size ks one can, again, use only m lookup adds. Moreover, the number of cluster centers is $(ks)^m$ with Q-PCPQ compared with k^m

for PQ. The increased cost is that the index size is $m \log(ks)$ bits per vector compared to $m \log(k)$ for PQ and the running time requires an additional skm floating point multiplications. Note that one could trivially increase the number of centers with PQ to $(ks)^m$ by using $k' = ks$ clusters in each section. However, with k typically taking values like 256, and s taking values like 16 and 32, the term $k'd = ksd$ in the query complexity will dominate the query time. Moreover, clustering vectors to $k' = 256 \times 32 \approx 7500$ is not usually feasible during index creation time, especially since the number of points indexed can be as large as 10^9 in large datasets. We compare the number of centers, application time and index size for these methods in Table 1.

Moreover, we show that the choice of the optimal centers and scaling coefficients for PCPQ and Q-PCPQ can be made to be loss aware. Following the logic in [18], one can weight the loss of $(\langle x_i, q \rangle - \langle \tilde{x}_i, q \rangle)^2$ higher if $\langle x_i, q \rangle$ is large and therefore x_i is a likely match for q . Taking that into account, one gets an anisotropic cost function for the optimal cluster centers. In our experiments we show that the additional flexibility afforded by the scalars in Q-APCPQ make its recall performance better than ScaNN on standard benchmark datasets for MIPS.

1.1 Related Works

Rotation matrix. In state-of-the-art implementations of PQ [14, 15, 18, 22, 44], typically, a rotation matrix $R \in \mathbb{R}^{d \times d}$ is applied to the data before performing clustering and applying PQ. The rotation matrix R is typically learned to make the data more suitable for breaking the d dimensions into sections in PQ. Several methods are used to learn and optimize the matrix R , including IPQ [15], OPQ [14] and MSQ [44]. Our methods address the method of clustering and performing the product quantization, and are oblivious to pre-processing – in particular, for a rotation matrix $R \in \mathbb{R}^{d \times d}$, we can approximate the inner-product $\langle x, q \rangle$ with $\sum_{i=1}^m \langle R\alpha_x^{(i)} c_x^{(i)}, Rq \rangle$ where $\alpha_x^{(i)}, c_x^{(i)}$ denotes the scaling and center from the i -th section of Q-PCPQ (or Q-APCPQ) for the data point x . A natural future direction to study is whether one can jointly learn the centers, scaling and rotation matrix in order to increase the performance of Q-PCPQ and Q-APCPQ.

Optimization methods. Several works have focused on proposing novel methods of finding the centers and the assignment of points to centers. For instance, LSQ [26] and LSQ++ [27] uses a local search based method that outperform the traditional, simpler alternating-minimization based methods. Some methods are proposed to optimize the quality of the centers by introducing cross-training across sections when finding centers, e.g. CompQ [30] is a stochastic gradient descent based method that achieves this by doing a joint training across sections and CQ [45] is a method that penalizes an error dependent on centers across sections. Our method introduces a novel clustering method, along with a optimization problem for PQ which we optimize using a simple alternating-minimization based approach. We leave the development of more advanced optimization methods for future work.

Non-PQ Methods. There are several works that approach MIPS using techniques different than PQ. One popular method is *locality sensitive hashing* LSH, which has seen a flurry of work [20, 29, 35, 36] for MIPS tasks. In addition, several recent works [10, 12, 21, 23, 33, 34] have looked at using a neural network to embed the input points and performing the search in the embedded space. Comparison of these methods against PQ methods, such as ours, is a vital research interest to better understand the performance of MIPS systems and we leave this to future work.

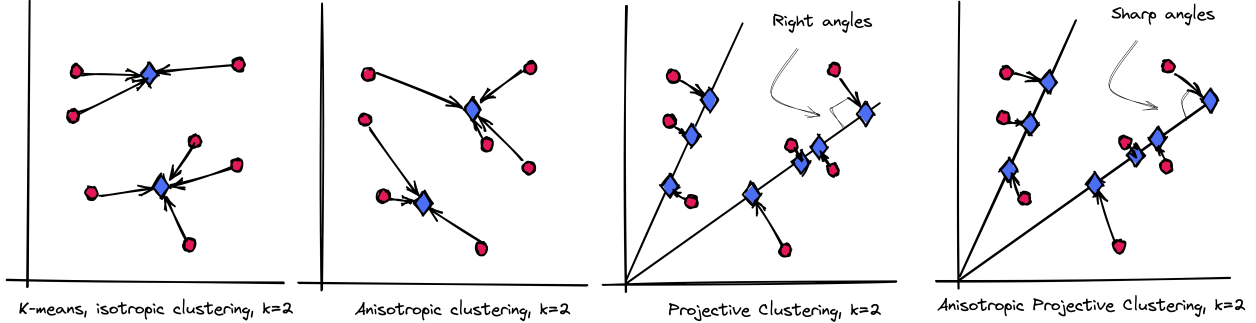


Figure 1: An illustration of k -clustering, projective k -clustering and their anisotropic counterparts for $k = 2$. While centers in k -clustering and anisotropic k -clustering are points, for their projective counterparts, they correspond to one-dimensional subspaces. Anisotropic projective clustering has the effect of pushing the centers further away from the origin.

1.2 Preliminaries

Throughout we denote $X \in \mathbb{R}^{n \times d}$ to be the matrix defined by the data points x_1, \dots, x_n and define $\bar{d} = d/m$ to be the dimension of each of the m sections of coordinates in PQ. We sometimes write $A \subseteq X$ to denote a subset A of the data points in X . Additionally, to define the quality of approximation from clustering for MIPS, we denote \mathcal{Q} to be a distribution over a set of queries in \mathbb{R}^d .

2 Projective Clustering

In projective k -clustering, our goal is to find $c_1, \dots, c_k \in \mathbb{R}^{\bar{d}}$ and scalars $\alpha_1, \dots, \alpha_n$ which minimize the following objective:

$$\min_{\substack{c_1, \dots, c_k \in \mathbb{R}^{\bar{d}} \\ \alpha_1, \dots, \alpha_n}} \sum_{i=1}^n \min_{j \in [k]} \mathbf{E}_{q \sim \mathcal{Q}} [(\langle q, x_i \rangle - \langle q, \alpha_i c_j \rangle)^2]. \quad (1)$$

When the query distribution \mathcal{Q} is isotropic, and α_i are constrained to the value 1.0, the above minimization problem reduces to the ubiquitous k -means clustering problem. When α_i are allowed to take on any real value, minimizing the loss function from (1) reduces to the popular k -projective clustering problem; see Appendix A.1 for proofs.

Definition 2.1. The k -projective clustering problem for points $X \in \mathbb{R}^{n \times \bar{d}}$ is a set of k points $c_1, \dots, c_k \in \mathbb{R}^{\bar{d}}$ such that the following is minimized

$$\min_{c_1, \dots, c_k \in \mathbb{R}^{\bar{d}}} \sum_{i=1}^n \min_{j \in [k]} \left\| x_i - \frac{\langle x_i, c_j \rangle}{\|c_j\|_2} \cdot c_j \right\|_2^2. \quad (2)$$

In words, the cost incurred by a point x is the cost of projecting it onto the direction (from the choice of k directions given by c_1, \dots, c_k) that minimizes the projection cost.

For a set of centers $c_1, \dots, c_k \in \mathbb{R}^{\bar{d}}$, and for each $j \in [k]$, let $X_j \subseteq X$ denote the set of all points in X that map to center c_j . For each X_j , denote $u_j, v_j \in \mathbb{R}^{\bar{d}}$ to be the top left and right singular vectors of X_j respectively and let $\sigma_j \in \mathbb{R}^{\geq 0}$ be the top singular value.

By the Eckhart-Young-Mirsky Theorem [11], we must have that $c_j = v_j$ and $X_j c_j = \sigma_j \cdot u_j$ for all $j \in [k]$ and hence, we can simplify the minimization problem from (2) as follows:

$$\begin{aligned}
\min_{\{c_j\}_{j=1}^k} \sum_{i=1}^n \min_{j \in [k]} \left\| x_i - \frac{\langle x_i, c_j \rangle}{\|c_j\|_2} \cdot c_j \right\|_2^2 &= \min_{\{c_j\}_{j=1}^k} \sum_{j=1}^k \sum_{x \in X_j} \left\| x - \frac{\langle x, c_j \rangle}{\|c_j\|_2} \cdot c_j \right\|_2^2 \\
&= \min_{\{X_j\}_{j=1}^k} \sum_{j=1}^k \sum_{x \in X_j} \|x - \sigma_j u_j v_j^\top\|_2^2 \\
&= \min_{\{X_j\}_{j=1}^k} \sum_{j=1}^k \|X_j - \sigma_j u_j v_j^\top\|_F^2 \\
&= \min_{\{X_j\}_{j=1}^k} \sum_{j=1}^k \|X_j\|_F^2 - \sigma_j^2 \\
&= \|X\|_F^2 - \max_{\{X_j\}_{j=1}^k} \sum_{j=1}^k \sigma_j^2
\end{aligned}$$

where the minimization over $\{X_j\}_{j=1}^k$ is a minimization over all partitions of the input X into k parts. It follows then that once the partition X_1, \dots, X_k is computed, the centers are given by $c_j = v_j$ for $j \in [k]$ and the optimal scalar α_i for the i -th point is the projection $\alpha_i = \sigma_j u_j v_j^\top$.

The running time of applying the projective clustering approximation is asymptotically identical to that of k -means and produces significantly more accurate results. This is unsurprising since projective clustering is more expressive than k -means. Moreover, the optimal solution for approximating a collection of vectors by a single vector is well known: it is the top singular vector of the collection of vectors rather than their geometric center, which is the optimal solution for k -means. Building on these encouraging results, we proceed to investigate the quantized version of projective clustering.

2.1 Quantized Projective k -Clustering

Recall that our goal is to quantize the projections $\alpha_1, \dots, \alpha_n$ of the points x_1, \dots, x_n to $s \in \mathbb{N}$ values. Given the centers c_1, \dots, c_k , we can write the quantized version of the minimization problem from above as follows.

Definition 2.2. In the *quantized projective k -clustering* problem, a partition $\{X_j\}_{j \in [k]}$ of the data X (corresponding to clusters) is given and the goal is to find a set of vectors $\{\bar{u}_j \in \mathbb{R}^{\bar{d}}\}_{j \in [k]}$ which contain at most s distinct entries while minimizing the following objective:

$$\min_{\{\bar{u}_j\}_{j \in [k]}} \sum_{j=1}^k \|X_j - \bar{u}_j v_j^\top\|_F^2 \tag{3}$$

where $v_j \in \mathbb{R}^{\bar{d}}$ is the top right singular vector of X_j .

It can be shown that in fact, the objective function from (3) is upper bounded by the cost of the optimal clustering plus the cost of doing a one-dimensional k -means clustering of the projections

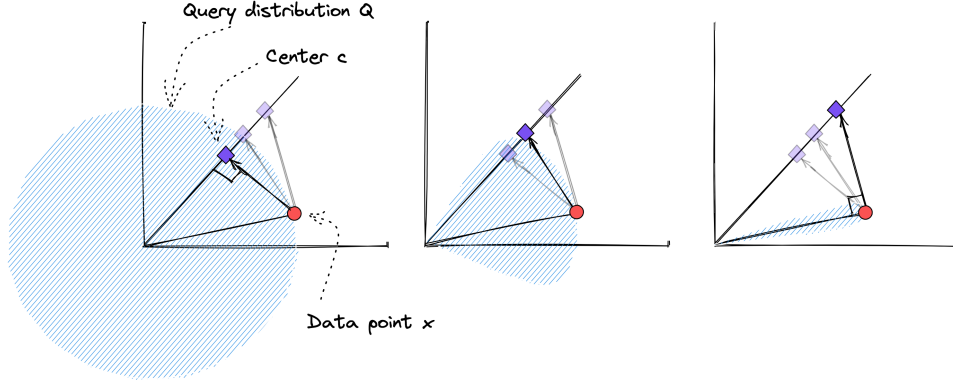


Figure 2: The optimal scaling α for anisotropic projective clustering with differing query distributions. The weight function $\mathbb{1}_t : \mathbb{R} \rightarrow \{0, 1\}$ essentially restricts the queries in the distribution \mathcal{Q} on which the loss $\langle q, x - c \rangle^2$ is measured by outputting 0 on all the queries q for which $\langle q, x \rangle < t$. When the distribution is isotropic, x is mapped to its projection. When $q = x$, the point x is mapped to a center c such that the inner-product $\langle c, q \rangle = \langle x, q \rangle = \|x\|_2^2$.

$\alpha_1, \dots, \alpha_n$ with $k = s$. We state this specifically in the following fact and give a proof in Appendix B.1.

Fact 2.3. *The loss in (3) is upper-bounded by:*

$$\min_{\{\bar{u}_j\}_{j \in [k]}} \sum_{j=1}^k \|X_j - \sigma_j u_j v_j^\top\|_F^2 + \|\sigma_j u_j - \bar{u}_j\|_2^2$$

where u_j and σ_j are the left singular vector and top singular value of X_j respectively.

It is now easy to see that minimizing the loss $\sum_{j=1}^k \|\sigma_j u_j - \bar{u}_j\|_2^2$ is simply a k -means problem in one dimension with $k = s$, hence this can be easily computed after finding the centers and the projections for each section.

3 Anisotropic Projective Clustering

The objective function in (1) takes the expectation over the entire query distribution \mathcal{Q} , however, as observed by Guo et al. [18], not all pairs of points and queries are equally important since in the MIPS setting we are interested in preserving the inner-product $\langle x, q \rangle$ only if it is large (and hence a candidate for a nearest neighbor). This observation motivates the work of Guo et al. [18] that introduces a weight function in the loss given by (1). Specifically, given a threshold $t > 0$, let $\mathbb{1}_t(x)$ be a weight function that is 1 when $x \geq t$ and 0 when $x < t$. Then, they consider the following *score-aware loss* function for clustering:

$$\min_{\substack{c_1, \dots, c_k \in \mathbb{R}^d \\ \alpha_1, \dots, \alpha_n}} \mathbf{E}_{q \sim \mathcal{Q}} \left[\sum_{i=1}^n \min_{j \in [k]} \mathbb{1}_t(\langle x_i, q \rangle) \cdot (\langle q, x_i \rangle - \langle q, \alpha_i c_j \rangle)^2 \right] \quad (4)$$

where α_i is fixed to be 1.0 and where $t > 0$ is a tuneable input-specific parameter¹. The threshold function $\mathbb{1}_t$ defines a cone of vectors (of unit length) around the point x_i . It essentially “selects” the queries from the support of \mathcal{Q} for which the inner-product between x_i and the queries should be preserved. Figure 1 depicts this intuition, showing that anisotropic (projective) clustering finds centers that have larger norm than in plain vanilla clustering so as to preserve the inner-products with the relevant queries, defined by the threshold function.

As shown in Guo et al. [18], the above loss (per point) can be written as a linear combination of the error introduced by the component of the residual $x_i - c_j$ that is parallel to x_i and the component that is orthogonal to x_i . Formally, define $r_{\parallel}(x, c) := x - \frac{\langle x, c \rangle}{\|x\|_2^2} x$ and $r_{\perp}(x, c) := \frac{\langle x, c \rangle}{\|x\|_2^2} x - c$, then, it was shown in Guo et al. [18, Theorem 3.2] that the loss in (4) is equivalent to minimizing the loss

$$\min_{c_1, \dots, c_k \in \mathbb{R}^{\bar{d}}} \sum_{i=1}^n \min_{j \in [k]} h_{\parallel}(\|x_i\|_2) \cdot \|r_{\parallel}(x, c_j)\|_2^2 + h_{\perp}(\|x_i\|_2) \cdot \|r_{\perp}(x, c_j)\|_2^2$$

where $h_{\parallel}(y) = (\bar{d} - 1) \int_0^{t/y} \sin^{\bar{d}-2} \theta - \sin^{\bar{d}} \theta d\theta$ and $h_{\perp}(y) = \int_0^{t/y} \sin^{\bar{d}} \theta d\theta$.

Intuitively, the functions h_{\parallel} and h_{\perp} represent how the error from the parallel component of the residual and the orthogonal component of the residual should be weighted depending on the weight-function $\mathbb{1}_t$ in the loss (4). It can be shown that for any $t \geq 0$ we have that $h_{\parallel} \geq h_{\perp}$, i.e. the parallel component of the error is weighted higher. We defer further discussion of h_{\parallel} and h_{\perp} to Appendix C.

A natural way to extend the above loss, as in projective k -clustering, is to remove the restriction on the value of $\alpha_1, \dots, \alpha_n$ and allow it to take on any real value. We term this the *anisotropic projective k -clustering problem* which we define below.

Definition 3.1. The *anisotropic projective k -clustering problem* for a set of points $X \in \mathbb{R}^{n \times \bar{d}}$ aims to find a set of k points $c_1, \dots, c_k \in \mathbb{R}^{\bar{d}}$ and n scalars $\alpha_1, \dots, \alpha_n \in \mathbb{R}$ such that the following is minimized

$$\min_{\substack{c_1, \dots, c_k \in \mathbb{R}^{\bar{d}} \\ \alpha_1, \dots, \alpha_n \in \mathbb{R}}} \sum_{i=1}^n \min_{j \in [k]} \left(h_{\parallel}(\|x_i\|_2) \cdot \|r_{\parallel}(x_i, \alpha_i c_j)\|_2^2 + h_{\perp}(\|x_i\|_2) \cdot \|r_{\perp}(x_i, \alpha_i c_j)\|_2^2 \right). \quad (5)$$

We show from a simple calculation that in fact, for a fixed c_j and x_i , one can compute the optimal $\alpha_i \in \mathbb{R}$ that minimizes the loss in (5). Intuitively, the optimal scaling pushes the center away from the projection in the direction of c_j depending on which queries have weight 1 in the loss function (5); Figure 2 depicts this intuition.

Fact 3.2. For vectors $x, c \in \mathbb{R}^{\bar{d}}$, we have

$$\operatorname{argmin}_{\alpha \in \mathbb{R}} h_{\parallel} \cdot \left\| x - \frac{\langle x, \alpha c \rangle}{\|x\|_2^2} x \right\|_2^2 + h_{\perp} \cdot \left\| \alpha c - \frac{\langle x, \alpha c \rangle}{\|x\|_2^2} x \right\|_2^2 = \frac{h_{\parallel} \cdot \langle x, c \rangle}{\frac{(h_{\parallel} - h_{\perp}) \langle x, c \rangle^2}{\|x\|_2^2} + h_{\perp} \cdot \|c\|_2^2}$$

where h_{\parallel} and h_{\perp} are abbreviations for $h_{\parallel}(\|x\|_2)$ and $h_{\perp}(\|x\|_2)$ respectively.

¹When the input is unit norm, it is suggested to set $t = 0.2$ [17, Section 3.2].

3.1 Quantized Anisotropic Projective Clustering

The quantized version of anisotropic projective k -clustering can be written by modifying the minimization problem from (5) like it was done for projective k -clustering. Specifically, given the centers c_1, \dots, c_k , the goal is to minimize the following loss:

$$\min_{\lambda_1, \dots, \lambda_s} \sum_{i=1}^n \min_{j \in [k], l \in [s]} \left(h_{\parallel}(\|x_i\|_2) \cdot \|r_{\parallel}(x_i, \lambda_l c_j)\|_2^2 + h_{\perp}(\|x_i\|_2) \cdot \|r_{\perp}(x_i, \lambda_l c_j)\|_2^2 \right). \quad (6)$$

Using the definition of r_{\parallel} and r_{\perp} , the term in the summation can be written in the form $w_i \lambda_l^2 + a_i \lambda_l + b_i$ where $w_i, a_i, b_i \in \mathbb{R}$ are constants² that are independent of $\lambda_1, \dots, \lambda_s$ and only dependent on the point x_i and the center it maps to. Hence, the above minimization problem can be simplified as follows:

$$\min_{\lambda_1, \dots, \lambda_s} \sum_{i=1}^n \min_{l \in [s]} w_i \lambda_l^2 + a_i \lambda_l + b_i.$$

Notice that this is a quadratic loss for s variables in one-dimension for which we can find a fixed point efficiently by doing an alternating minimization (with random initialization) since the minimization problem can be solved exactly for a single scalar.

4 Efficient Algorithms and Application to PQ

In this section we show how to implement Q-PCPQ and Q-APCPQ in two stages: first we give efficient algorithms in Section 4.2 and 4.2 to compute the centers and scalars for projective k -clustering (PCPQ) and anisotropic projective k -clustering (APCPQ) respectively, and then, in Section 4.3, we state how to create the index for Q-PCPQ and Q-APCPQ by using the methods from Section 2.1 and 3.1 to quantize the scalars we computed and store the mapping of the points to their respective centers and quantized scalars. In the same section, we show how the index for Q-PCPQ and Q-APCPQ is used to compute the inner-product between a query vector and every point.

Our main approach to compute the centers and scalars is to use an alternating-minimization algorithm to minimize the loss function (2) for PCPQ and (5) for APCPQ. Alternating-minimization has been a long-standing approach on finding the clustering in the literature for product quantization [14, 15, 18, 44].

4.1 Projective k -clustering

The projective k -clustering problem is a NP-Hard problem for $k \geq 2$ even in the 2D-plane, i.e. $\bar{d} = 2$. Nevertheless, several lines of work have proposed fast approximation algorithms – including algorithms inspired by Lloyd’s algorithm for k -means that iteratively find k one-dimensional subspaces [2], a monte-carlo sampling method [32] and coresets based algorithms [13, 37] that sample (and reweight) a small subset of the input points in such a way that the cost of clustering the subset of points is approximately the same as clustering the entire input, allowing the use of any black-box

² $w_i = (h_{\parallel} + h_{\perp})\langle x_i, c_j \rangle (\langle x_i, c_j \rangle - 2) + h_{\perp} \|c_j\|_2^2$, $a_i = -2\langle x_i, c_j \rangle$ and $b_i = h_{\parallel} \|x_i\|_2^2$.

algorithm (that is potentially computationally intractable on large datasets) on the much smaller set of points.

The algorithm we propose is similar to Lloyd’s algorithm and iterates between an *assignment step* and a *center finding step* – in each round the algorithm i) maps the points to the closest center by projecting every point to each of the directions (given by the centers) and picks the one that minimizes the squared distance of the point to its projection and ii) for each center, the algorithm considers all the points that mapped to the center in step i) and computes the top-right singular vector of those points to be the new center. It is easy to see from the Eckart-Young-Mirsky Theorem [11] that the top-right singular vector in fact minimizes the loss from (2) when $k = 1$.

Formally, we consider the following iterative procedure:

1. (Initialization) Sample k random points c_1, \dots, c_k from the data X .
2. (Assignment) For each point $x \in X$: let $j^* = \operatorname{argmin}_{j \in [k]} \|x - \frac{\langle x, c_j \rangle}{\|c_j\|_2^2} c_j\|_2$, set $\alpha_i = \frac{\langle x, c_{j^*} \rangle}{\|c_{j^*}\|_2^2}$ and assign c_{j^*} to be the center of x .
3. (Center Finding) For each $j \in [k]$: denote $X_j \subset X$ be the subset of the points that were assigned to center j in Step 2, compute the top-right singular vector v of X_j , i.e. $v = \operatorname{argmin}_{\|y\|=1} \|X_j - X_j y y^\top\|_F^2$, and set $c_j = v$.
4. (Termination) Repeat Step 2 and 3 until convergence or a maximum number of iterations has been reached.

Initialization. In practice, as in our experiments, we can hope to find better solutions (centers) by initializing the centers using an off-the-shelf algorithm for another clustering problem, like k -means++. Recently, the work of [37] proposed a different initialization that provably produces a $O(\log(k))$ -approximation for the projective k -clustering problem. The algorithm first normalizes all the points in X so they have unit norm and then samples k points with a slight variant of the k -means++ initialization algorithm – specifically, the algorithm maintains a set S and, for k iterations, samples a point $x \in X \setminus S$ to add to S with probability proportional to $\min(\min_{s \in S} \|x - s\|_2^2, \min_{s \in S} \|x + s\|_2^2)$. Empirically, on the datasets we use, we found that initializing the centers with k -means++ produces centers with similar loss as this algorithm while being able to take advantage of optimized implementations of k -means++ leading to significant gains in indexing time.

4.2 Anisotropic Projective k -clustering

We propose an alternating-minimization framework for anisotropic projective k -clustering, similar to the algorithm from Section 4.1. The difference lies in the assignment stage, where we need to compute the optimal α_i for each data point $x_i \in X$ with respect to the anisotropic projective clustering loss from Definition 3.1 and in the center finding stage where, for each subset of points in X that are mapped to the same center, we need to compute the center that minimizes the aforementioned loss.

We showed in Fact 3.2 that computing the optimal α_i for each x_i can be done when the centers are fixed. It is left then to show how to compute the centers in the center finding stage ($k = 1$). Guo et al. [18] show that when $\alpha_i = 1$, there is a closed form solution to finding the center that

minimizes the loss from Definition 3.1. A simple adaptation of their proof gives us a closed form solution to the aforementioned loss when α_i is any arbitrary fixed scalar.

Theorem 4.1 (Theorem 4.2, [18]). *For n points $X \in \mathbb{R}^{n \times \bar{d}}$, we have that*

$$c^* := \left(\sum_{i=1}^n \frac{\alpha_i^2 (h_{\parallel,i} - h_{\perp,i})}{\|x_i\|_2^2} x_i x_i^\top + I \cdot \alpha_i^2 h_{\perp,i} \right)^{-1} \sum_{i=1}^n \alpha_i h_{\parallel,i} x_i$$

is the solution to the minimization problem $\operatorname{argmin}_{c \in \mathbb{R}^{\bar{d}}} \sum_{i=1}^n h_{\parallel,i} \|r_{\parallel}(x_i, \alpha_i c)\|_2^2 + h_{\perp,i} \|r_{\perp}(x_i, \alpha_i c)\|_2^2$ and where $h_{\parallel,i}$ and $h_{\perp,i}$ are abbreviations for $h_{\parallel}(\|x_i\|_2)$ and $h_{\perp}(\|x_i\|_2)$ respectively.

We propose the following iterative procedure for the anisotropic projective k -clustering problem.

1. (Initialization) Sample k random points c_1, \dots, c_k from the data X .
2. (Assignment) For each point $x_i \in X$: compute $\beta_i[j] := h_{\parallel,i} \langle x_i, c_j \rangle \left(\frac{(h_{\parallel,i} - h_{\perp,i}) \langle x_i, c_j \rangle^2}{\|x_i\|_2^2} + h_{\perp,i} \cdot \|c_j\|_2^2 \right)^{-1}$ for each $j \in [k]$. Compute $j^* = \operatorname{argmin}_{j \in [k]} \|x_i - \beta_i[j] c_j\|_2$, then, set $\alpha_i = \beta_i[j^*]$ and c_{j^*} to be the center for x_i .
3. (Center Finding) For each $j \in [k]$: denote $X_j \subset X$ be the subset of the points that were assigned to center j in Step 2, set c_j to be

$$\left(\sum_{\substack{i \in [n] \text{ s.t.} \\ x_i \in X_j}} \frac{\alpha_i^2 (h_{\parallel,i} - h_{\perp,i})}{\|x_i\|_2^2} x_i x_i^\top + I \cdot \alpha_i^2 h_{\perp,i} \right)^{-1} \sum_{\substack{i \in [n] \text{ s.t.} \\ x_i \in X_j}} \alpha_i h_{\parallel,i} \cdot x_i$$

4. (Termination) Repeat Step 2 and 3 until convergence or a maximum number of iterations has reached.

Notice that unlike in our algorithm for projective k -clustering, the center finding stage in the above algorithm does not find the optimal scaling and center for each subset (cluster) of points. Instead we solve the anisotropic k -clustering problem on the cluster and then compute the optimal scaling using Fact 3.2. Computing the optimal scaling and center jointly, like we did for vanilla projective clustering, is an open problem we leave for future work.

4.3 Product Quantization and Running Time

Next, we outline how we use the algorithms from Sections 4.1 and 4.2 to compute the index for Q-PCPQ and Q-APCPQ respectively and how the inner-product of the query vector with each point is computed during query time.

As discussed in Section 1, the columns of the input data $X \in \mathbb{R}^{n \times d}$ are split into m contiguous chunks $X^{(1)}, \dots, X^{(m)} \in \mathbb{R}^{n \times d/m}$ where $X^{(j)}$ contains the coordinates $[jm, \dots, (j+1)m - 1]$. We then compute the centers $C^{(1)}, \dots, C^{(m)} \in \mathbb{R}^{k \times d/m}$ and scalars $\{\alpha_i^{(j)} : j \in [m], i \in [n]\}$ independently for each section $j \in [m]$. The centers and scalars for each section are computed using the method in Section 4.1 for Q-PCPQ and in Section 4.2 for Q-APCPQ.

We store m lookup tables $\{\phi_j : [n] \rightarrow [k] \mid j \in [m]\}$, where lookup table ϕ_j maps every point to its center in $C^{(j)}$.

In order to quantize the scalars, we follow the procedure from Section 2.1 for Q-PCPQ and Section 3.1 for Q-APCPQ³. Specifically, the scalars $\{\alpha_i^{(j)} \mid j \in [m], i \in [n]\}$ are themselves quantized to s values $\{\lambda_1, \dots, \lambda_s\}$ using the aforementioned procedure and m mappings $\{\gamma_j : [n] \rightarrow [s] \mid j \in [m]\}$ are created such that mapping γ_j maps the scalars $\{\alpha_i^{(j)}\}_{i \in [n]}$ from section j to their respective quantized scalar among $\{\lambda_1, \dots, \lambda_s\}$.

Inner-product computation. For a query $q \in \mathbb{R}^d$, let $[q_1, \dots, q_m]$ denote the m sections of the coordinates of q each containing d/m coordinates. The inner-products between the data X and q is computed in the following phases:

- i. for each $j \in [m]$, the k -length vector $\eta_j := C^{(j)}q_j$ is computed, then,
- ii. for each $j \in [m]$ and $l \in [s]$, the quantity $\eta_j \cdot \lambda_l$ is computed and stored in a lookup table of size skm , and finally,
- iii. to compute the inner-product with x_i , the sum

$$\sum_{j=1}^m \eta_{j, \phi_j(i)} \cdot \lambda_{\gamma_j(i)} \tag{7}$$

is computed by performing m lookups, one for each term.

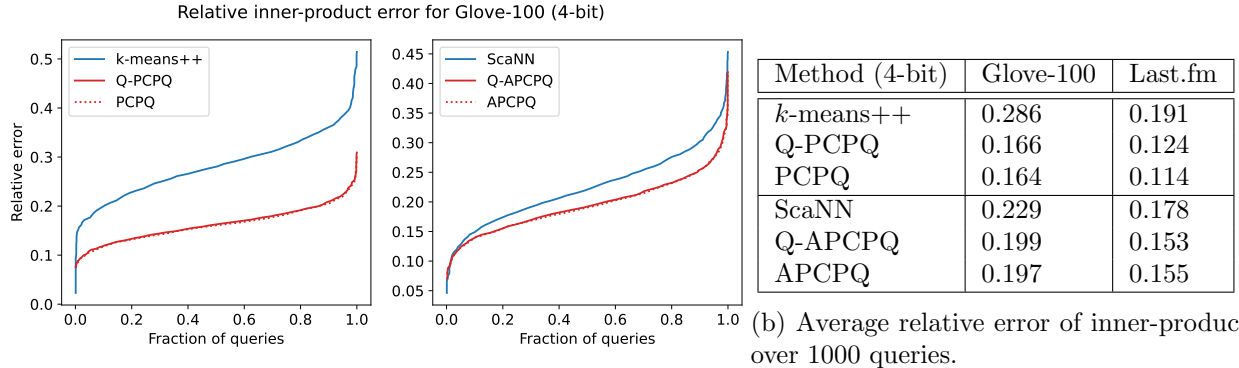
Running time and space complexity. Computing the inner-products of the centers in each section with q (i.e. stage i.) takes kd multiply-adds, since each section has d/m coordinates and there are m sections with k centers each. Computing the products with the s scalars $\lambda_1, \dots, \lambda_s$ requires skm multiplication operations, k for each scalar and section. And finally computing the inner-product in step iii. requires m lookups and m additions per point, for a total of nm lookups and additions. In total, the complexity of the search is $kd + skm + 2nm$ operations.

Storing the mapping $\phi^{(1)}, \dots, \phi^{(m)}$ requires $m \log_2(k)$ bits per point and storing the scalar quantizing requires $\log_2(s)$ bits per point, leading to a total of $n(m \log_2(k) + \log_2(s))$ bits to store the index. In addition, $kd + s$ floating point integers need to be stored, which is a lower order term since $n \gg kd/m$.

5 Experiments

In this section we compare between k -clustering and its projective counterparts we proposed on their performance for maximum inner-product search. Specifically, we consider k -means++ and

³Recent implementations of product quantization for Euclidean distance [44] and that of anisotropic k -clustering (ScaNN) [18] unit normalize all the data and store the norm $\|x_i\|_2$ as a scalar α_i for each x_i separately. The scalars are then quantized to s values, and during query time, the inner-product computations for each point are scaled by its respective quantized norm.



(a) Relative error of each method over 1000 queries, sorted by the magnitude of the error with the query.

Figure 3: Comparison of 4-bit *k*-means++, ScaNN, Q-PCPQ and Q-APCPQ (along with the versions without scalar quantization: PCPQ and APCPQ) on the relative error of approximating the top inner-product over 1000 queries on Glove-100 and Last.fm.

anisotropic *k*-clustering (ScaNN) [18] and compare them to quantized projective *k*-clustering (Q-PCPQ) and quantized anisotropic projective *k*-clustering (Q-APCPQ). In addition, we add the comparisons to the versions of projective clustering without quantizing the scalars, which we denote by PCPQ and APCPQ respectively. In fixed-bit-rate settings we analyze the retrieval performance (i.e. recall) and the quality of approximation of maximum inner-product values to show that Q-PCPQ and Q-APCPQ achieve significantly better performance on both measures in standard benchmark datasets for MIPS.

Datasets. We use Glove-100 introduced in Pennington et al. [31] which is a collection of 1.2 million word embeddings in 100-dimensions. Glove-100 is used in Guo et al. [18] and is also one of the main benchmarks in Aumüller et al. [4] for inner-product search; Aumüller et al. [4] is a widely-used tool for benchmarking approximate nearest neighbor algorithms. While Glove-100 is meant for cosine similarity search, we unit-normalize all the points at training time making MIPS equivalent to cosine similarity. Additionally we use the Last.fm dataset, another benchmark dataset from Aumüller et al. [4] for MIPS, containing 300,000 points in 65-dimensions created by embedding soundtracks using a matrix factorization based recommendation model for music.

Multiscale quantization. Performing PQ on the entire dataset when the dataset has more than 10^6 data points can lead to poor performance and can be prohibitive for datasets of size 10^7 or 10^9 . In order to circumvent this, typically in similarity search systems [18, 22, 44] an initial clustering of the dataset is done, followed by a product quantization of the data points in each cluster.

Usually, like in the aforementioned results, the residuals of the data points in each cluster are used for the PQ instead of the data points themselves. Specifically, for data points $X \in \mathbb{R}^{n \times d}$ a parameter $\bar{k} \in \mathbb{N}$ is chosen and \bar{k} cluster centers $c_1, \dots, c_{\bar{k}} \in \mathbb{R}^d$ are computed. Typically \bar{k} is chosen to be around $O(\sqrt{n})$ in order to balance the accuracy-performance tradeoff⁴. Each point in X is then mapped to its closest cluster center (in ℓ_2 -distance) to obtain a clustering $\{\mathcal{C}_1, \dots, \mathcal{C}_{\bar{k}}\}$

⁴see <https://github.com/facebookresearch/faiss/wiki/Guidelines-to-choose-an-index>

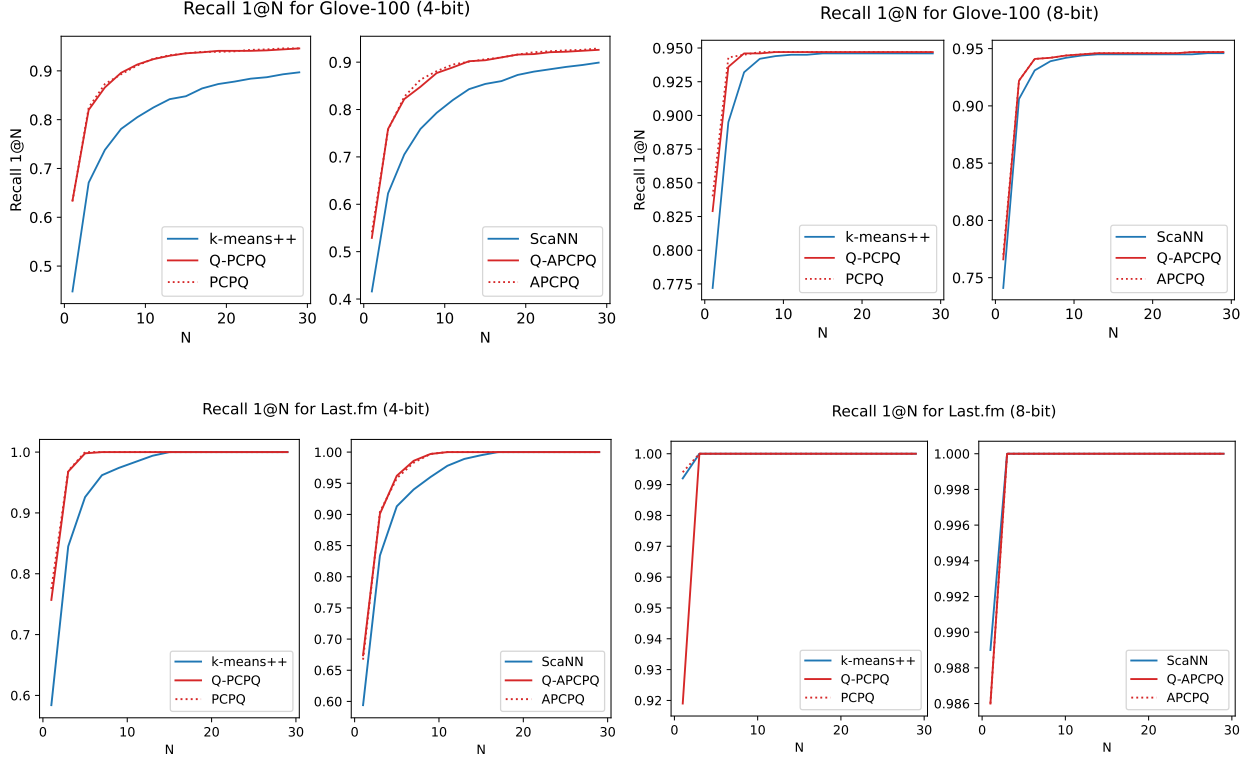


Figure 4: Comparison of k -means++ and ScaNN with Q-PCPQ and Q-APCPQ (and without projective quantization: PCPQ and APCPQ) respectively on Recall1@N on Glove-100 and Last.fm datasets in the 4-bit and 8-bit settings.

that partitions X . Finally, in order to build the index, the PQ method is applied to each cluster $\mathcal{C}_1, \dots, \mathcal{C}_{\bar{k}}$ separately.

For queries, a parameter $k_{\text{probe}} \ll \bar{k}$ parameter is picked beforehand. On the arrival of a query $q \in \mathbb{R}^d$, points in the top k_{probe} clusters are queried based on the ordering of $\langle q, c_1 \rangle, \dots, \langle q, c_{\bar{k}} \rangle$ to obtain the point(s) with maximum inner-product with q .

Parameters. For each dataset, we compute the initial clustering of \bar{k} clusters using the `scikit-learn` implementation of k -means++ and set \bar{k} so that $n/\bar{k} \approx 1000$. This provides a fair comparison for the retrieval performance and inner-product approximation of the PQ methods across datasets. For each dataset, the same clustering is used across all compared methods and parameters.

We investigate two regimes for k , i.e., the number of centers in each section: $k = 16$ and $k = 256$ which are denoted the 4-bit and 8-bit settings respectively. We set the number of sections m to be $m = 25$ for Glove-100 and $m = 16$ for Last.fm, this leads to $\bar{d} = 4$ coordinates per section. In the projected quantization setting (Q-PCPQ and Q-APCPQ), we set the scalar quantization to be $s = 8$.

For ScaNN and Q-APCPQ (and APCPQ), we set the threshold in the weight function to be $0.2 \times$ (average ℓ_2 -norm of the input vectors). An in-depth discussion of the rationale behind setting this threshold is done in Guo et al. [18].

Method	Glove-100				Last.fm			
	Recall 1@1		Recall 1@10		Recall 1@1		Recall 1@10	
	4-bit	8-bit	4-bit	8-bit	4-bit	8-bit	4-bit	8-bit
<i>k</i> -means++	0.448	0.772	0.825	0.945	0.584	0.992	0.984	1.000
Q-PCPQ	0.633	0.829	0.924	0.947	0.775	0.919	1.000	1.000
PCPQ	0.634	0.840	0.925	0.947	0.757	0.994	1.000	1.000
ScaNN	0.416	0.741	0.820	0.944	0.594	0.989	0.978	1.000
Q-APCPQ	0.529	0.766	0.889	0.945	0.667	0.986	1.000	1.000
APCPQ	0.541	0.770	0.895	0.945	0.674	0.986	1.000	1.000

Table 2: Recall1@1 and Recall1@10 values for *k*-means++, ScaNN, Q-PCPQ (and PCPQ) and Q-APCPQ (and APCPQ) for Glove-100 and Last.fm (averaged over 1000 queries) in the 4-bit and 8-bit regimes.

Setup. Our implementations for the methods are in Python v3.x and all our experiments were run on `n1-standard` Google Cloud Engine VMs with 4vCPUs @2.2GHz and 15GB RAM.

5.1 Approximating maximum inner-product

We compare the methods on their accuracy of estimating the top-1 inner-product. Specifically, we measure the relative error $|\langle q, x_i \rangle - \sum_{j=1}^m \eta_{j, \phi_j(i)} \cdot \lambda_{\gamma(i)}| / |\langle q, x_i \rangle|$ for the point x_i with the highest inner-product with q over 1000 such queries. Here the summation $\sum_{j=1}^m \eta_{j, \phi_j(i)} \cdot \lambda_{\gamma(i)}$ is the approximate inner-product for query q from (7). We perform a head-to-head comparison of each method in the 4-bit setting: i) *k*-means++ against Q-PCPQ (and PCPQ), and ii) ScaNN against Q-APCPQ (and APCPQ). The results over the 1000 queries are shown in Figure 3a and the average relative error is given in Table 3b.

The results show that Q-PCPQ and Q-APCPQ consistently approximate the top inner-product with the query better than *k*-means++ and ScaNN respectively. Specifically, the relative error is 12% and 3% lower for Q-PCPQ and Q-APCPQ respectively compared to their non-projective counterparts on Glove-100. Additionally, the results show that the loss in the approximation of the inner-product from quantizing the projections is negligible; as seen by the average relative errors between PCPQ and Q-PCPQ (and between APCPQ and Q-APCPQ) in Table 3b.

While Q-APCPQ does better on average than ScaNN, the average relative error is worse for Q-APCPQ than for Q-PCPQ. This does not align with the rationale of using the score-aware loss from (4), since the score-aware loss is meant to approximate top inner-products better than its counterpart in (1) that is not score-aware. We suspect that this might be due to the fact that we do not solve the minimization problem given in (5) for the anisotropic projective *k*-clustering optimally when $k = 1$.

5.2 Recall

One of the most important measures of the performance of a MIPS system is its retrieval performance. Specifically, for a set of queries Q and a parameter $N \in \mathbb{N}^+$, let $\pi_N(q)$ be the top- N points based on the approximate inner-products computed by method under consideration. Then, the

Recall1@N for the set of queries Q is the following quantity:

$$\text{Recall1@N} = \frac{1}{|Q|} \sum_{q \in Q} \mathbf{1} \left[\max_{x \in \pi_N(q)} \langle x, q \rangle \geq \max_{x \in X} \langle x, q \rangle \right].$$

We compare the performance of each method in 4-bit and 8-bit settings and measure the Recall1@1 and Recall1@10 for each dataset in Table 2. Figure 4 plots the Recall1@N for Glove-100 and Last.fm in the 4-bit and 8-bit setting. Especially in the 4-bit setting, we see that Q-PCPQ and Q-APCPQ achieve significant recall gains over their non-projective counterparts (k -means++ and ScaNN); achieving approximately 8% – 10% recall gains in the anisotropic setting for Recall1@1 and close to 19% gain for Q-PCPQ in the same setting!

In the 8-bit regime, the number of centers per section is comparable to the number of data points, i.e., $k = 256$ for 1000 points. Hence, even vanilla k -means++ clustering fits the data very well, achieving as little as 3.16% reconstruction error on Glove-100. In this setting we have that $k \approx n$, precluding the need for product quantization in the first place. This could explain the fact that Q-PCPQ and Q-APCPQ have much more modest gains in the 8-bit regime, and even does worse on Recall1@1 on Last.fm in the 8-bit regime. On much larger datasets however, where the number of centers k per section is much smaller than the number of points being indexed, we expect Q-PCPQ to do much better than k -means, as is consistently shown in the 4-bit regime, where k -means++ achieves 30.09% reconstruction error on Glove-100.

References

- [1] Pinecone: Vector database for similarity search. URL <https://www.pinecone.io/>.
- [2] Pankaj K Agarwal and Nabil H Mustafa. K -means projective clustering. In *Proceedings of the twenty-third ACM SIGMOD-SIGACT-SIGART Symposium on Principles of Database Systems*, pages 155–165, 2004.
- [3] Alexandr Andoni, Piotr Indyk, Thijs Laarhoven, Ilya Razenshteyn, and Ludwig Schmidt. Practical and optimal lsh for angular distance. In C. Cortes, N. Lawrence, D. Lee, M. Sugiyama, and R. Garnett, editors, *Advances in Neural Information Processing Systems*, volume 28. Curran Associates, Inc., 2015.
- [4] Martin Aumüller, Erik Bernhardsson, and Alexander Faithfull. Ann-benchmarks: A benchmarking tool for approximate nearest neighbor algorithms. In *International Conference on Similarity Search and Applications*, pages 34–49. Springer, 2017.
- [5] Moses S Charikar. Similarity estimation techniques from rounding algorithms. In *Proceedings of the thirty-fourth annual ACM symposium on Theory of computing*, pages 380–388, 2002.
- [6] Qi Chen, Haidong Wang, Mingqin Li, Gang Ren, Scarlett Li, Jeffery Zhu, Jason Li, Chuanjie Liu, Lintao Zhang, and Jingdong Wang. Sptag: A library for fast approximate nearest neighbor search, 2018. URL <https://github.com/Microsoft/SPTAG>.
- [7] Paolo Cremonesi, Yehuda Koren, and Roberto Turrin. Performance of recommender algorithms on top-n recommendation tasks. In *Proceedings of the fourth ACM conference on Recommender systems*, pages 39–46, 2010.

- [8] Sanjoy Dasgupta and Yoav Freund. Random projection trees and low dimensional manifolds. In *Proceedings of the fortieth annual ACM symposium on Theory of computing*, pages 537–546, 2008.
- [9] Thomas Dean, Mark A Ruzon, Mark Segal, Jonathon Shlens, Sudheendra Vijayanarasimhan, and Jay Yagnik. Fast, accurate detection of 100,000 object classes on a single machine. In *Proceedings of the IEEE Conference on Computer Vision and Pattern Recognition*, pages 1814–1821, 2013.
- [10] Yihe Dong, Piotr Indyk, Ilya Razenshteyn, and Tal Wagner. Learning space partitions for nearest neighbor search. In *International Conference on Learning Representations*, 2020.
- [11] Carl Eckart and Gale Young. The approximation of one matrix by another of lower rank. *Psychometrika*, 1(3):211–218, 1936.
- [12] Venice Erin Liong, Jiwen Lu, Gang Wang, Pierre Moulin, and Jie Zhou. Deep hashing for compact binary codes learning. In *Proceedings of the IEEE Conference on Computer Vision and Pattern Recognition*, pages 2475–2483, 2015.
- [13] Dan Feldman, Melanie Schmidt, and Christian Sohler. Turning big data into tiny data: Constant-size coresets for k-means, pca, and projective clustering. *SIAM Journal on Computing*, 49(3):601–657, 2020.
- [14] Tiezheng Ge, Kaiming He, Qifa Ke, and Jian Sun. Optimized product quantization for approximate nearest neighbor search. In *Proceedings of the IEEE Conference on Computer Vision and Pattern Recognition*, pages 2946–2953, 2013.
- [15] Yunchao Gong, Svetlana Lazebnik, Albert Gordo, and Florent Perronnin. Iterative quantization: A procrustean approach to learning binary codes for large-scale image retrieval. *IEEE Transactions on Pattern Analysis and Machine Intelligence*, 35(12):2916–2929, 2012.
- [16] Mihajlo Grbovic and Haibin Cheng. Real-time personalization using embeddings for search ranking at airbnb. In *Proceedings of the 24th ACM SIGKDD International Conference on Knowledge Discovery & Data Mining*, pages 311–320, 2018.
- [17] Ruiqi Guo, Sanjiv Kumar, Krzysztof Choromanski, and David Simcha. Quantization based fast inner product search. In *Artificial Intelligence and Statistics*, pages 482–490. PMLR, 2016.
- [18] Ruiqi Guo, Philip Sun, Erik Lindgren, Quan Geng, David Simcha, Felix Chern, and Sanjiv Kumar. Accelerating large-scale inference with anisotropic vector quantization. In *International Conference on Machine Learning*, pages 3887–3896. PMLR, 2020.
- [19] Ben Harwood and Tom Drummond. Fanng: Fast approximate nearest neighbour graphs. In *Proceedings of the IEEE Conference on Computer Vision and Pattern Recognition*, pages 5713–5722, 2016.
- [20] Qiang Huang, Guihong Ma, Jianlin Feng, Qiong Fang, and Anthony KH Tung. Accurate and fast asymmetric locality-sensitive hashing scheme for maximum inner product search. In *Proceedings of the 24th ACM SIGKDD International Conference on Knowledge Discovery & Data Mining*, pages 1561–1570, 2018.

- [21] Himalaya Jain, Joaquin Zepeda, Patrick Pérez, and Rémi Gribonval. Subic: A supervised, structured binary code for image search. In *Proceedings of the IEEE International Conference on Computer Vision*, pages 833–842, 2017.
- [22] Jeff Johnson, Matthijs Douze, and Hervé Jégou. Billion-scale similarity search with gpus. *IEEE Transactions on Big Data*, 2019.
- [23] Benjamin Klein and Lior Wolf. End-to-end supervised product quantization for image search and retrieval. In *Proceedings of the IEEE/CVF Conference on Computer Vision and Pattern Recognition*, pages 5041–5050, 2019.
- [24] Xiaoyun Li and Ping Li. Random projections with asymmetric quantization. In *NeurIPS*, pages 10857–10866, 2019.
- [25] Yu A Malkov and Dmitry A Yashunin. Efficient and robust approximate nearest neighbor search using hierarchical navigable small world graphs. *IEEE transactions on pattern analysis and machine intelligence*, 42(4):824–836, 2018.
- [26] Julieta Martinez, Joris Clement, Holger H Hoos, and James J Little. Revisiting additive quantization. In *European Conference on Computer Vision*, pages 137–153. Springer, 2016.
- [27] Julieta Martinez, Shobhit Zakhmi, Holger H Hoos, and James J Little. Lsq++: Lower running time and higher recall in multi-codebook quantization. In *Proceedings of the European Conference on Computer Vision (ECCV)*, pages 491–506, 2018.
- [28] Marius Muja and David G Lowe. Scalable nearest neighbor algorithms for high dimensional data. *IEEE transactions on pattern analysis and machine intelligence*, 36(11):2227–2240, 2014.
- [29] Behnam Neyshabur and Nathan Srebro. On symmetric and asymmetric lshs for inner product search. In *International Conference on Machine Learning*, pages 1926–1934. PMLR, 2015.
- [30] Ezgi Can Ozan, Serkan Kiranyaz, and Moncef Gabbouj. Competitive quantization for approximate nearest neighbor search. *IEEE Transactions on Knowledge and Data Engineering*, 28(11):2884–2894, 2016.
- [31] Jeffrey Pennington, Richard Socher, and Christopher D Manning. Glove: Global vectors for word representation. In *Proceedings of the 2014 Conference on Empirical Methods in Natural Language Processing (EMNLP)*, pages 1532–1543, 2014.
- [32] Cecilia M Procopiuc, Michael Jones, Pankaj K Agarwal, and TM Murali. A monte carlo algorithm for fast projective clustering. In *Proceedings of the 2002 ACM SIGMOD International Conference on Management of Data*, pages 418–427, 2002.
- [33] Alexandre Sablayrolles, Matthijs Douze, Nicolas Usunier, and Hervé Jégou. How should we evaluate supervised hashing? In *2017 IEEE International Conference on Acoustics, Speech and Signal Processing (ICASSP)*, pages 1732–1736. IEEE, 2017.
- [34] Alexandre Sablayrolles, Matthijs Douze, Cordelia Schmid, and Hervé Jégou. Spreading vectors for similarity search. In *International Conference on Learning Representations*, 2019.
- [35] Anshumali Shrivastava and Ping Li. Asymmetric lsh (alsh) for sublinear time maximum inner product search (mips). In Z. Ghahramani, M. Welling, C. Cortes, N. Lawrence, and K. Q. Weinberger, editors, *Advances in Neural Information Processing Systems*, volume 27. Curran Associates, Inc., 2014.

- [36] Anshumali Shrivastava and Ping Li. Improved asymmetric locality sensitive hashing (alsh) for maximum inner product search (mips). In *UAI*, pages 812–821. Citeseer, 2015.
- [37] Adiel Statman, Liat Rozenberg, and Dan Feldman. Faster projective clustering approximation of big data. *arXiv preprint arXiv:2011.13476*, 2020.
- [38] Santosh S Vempala. *The random projection method*, volume 65. American Mathematical Soc., 2005.
- [39] Thanh Vu, Dat Quoc Nguyen, Mark Johnson, Dawei Song, and Alistair Willis. Search personalization with embeddings. In Joemon M Jose, Claudia Hauff, Ismail Sengor Altıngövdü, Dawei Song, Dyaa Albakour, Stuart Watt, and John Tait, editors, *Advances in Information Retrieval*, pages 598–604, Cham, 2017. Springer International Publishing.
- [40] Bin Wang, Zhiwei Li, Mingjing Li, and Wei-Ying Ma. Large-scale duplicate detection for web image search. In *2006 IEEE International Conference on Multimedia and Expo*, pages 353–356. IEEE, 2006.
- [41] Meng Wang, Kuiyuan Yang, Xian-Sheng Hua, and Hong-Jiang Zhang. Towards a relevant and diverse search of social images. *IEEE Transactions on Multimedia*, 12(8):829–842, 2010.
- [42] Jason Weston, Samy Bengio, and Nicolas Usunier. Large scale image annotation: learning to rank with joint word-image embeddings. *Machine learning*, 81(1):21–35, 2010.
- [43] Ledell Yu Wu, Adam Fisch, Sumit Chopra, Keith Adams, Antoine Bordes, and Jason Weston. Starspace: Embed all the things! In *Thirty-Second AAAI Conference on Artificial Intelligence*, 2018.
- [44] Xiang Wu, Ruiqi Guo, Ananda Theertha Suresh, Sanjiv Kumar, Daniel N Holtmann-Rice, David Simcha, and Felix Yu. Multiscale quantization for fast similarity search. *Advances in Neural Information Processing Systems*, 30:5745–5755, 2017.
- [45] Ting Zhang, Chao Du, and Jingdong Wang. Composite quantization for approximate nearest neighbor search. In *International Conference on Machine Learning*, pages 838–846. PMLR, 2014.
- [46] Wengang Zhou, Houqiang Li, and Qi Tian. Recent advance in content-based image retrieval: A literature survey. *arXiv preprint arXiv:1706.06064*, 2017.

A Projective Clustering

Lemma A.1. *When \mathcal{Q} is isotropic over $\mathbb{R}^{\bar{d}}$, we have that*

$$\min_{c_1, \dots, c_k \in \mathbb{R}^{\bar{d}}} \sum_{i=1}^n \min_{\alpha \in \mathbb{R}, j \in [k]} \mathbf{E}_{q \sim \mathcal{Q}} \left[\langle q, x - \alpha \cdot c_j \rangle^2 \right] = \min_{c_1, \dots, c_k \in \mathbb{R}^{\bar{d}}} \sum_{i=1}^n \min_{j \in [k]} \left\| x_i - \frac{\langle x_i, c_j \rangle}{\|c_j\|_2} \cdot c_j \right\|_2^2.$$

Proof.

$$\min_{c_1, \dots, c_k} \sum_{i=1}^n \min_{\alpha, j} \mathbf{E}_{q \sim \mathcal{Q}} \left[\langle q, x - \alpha \cdot c_j \rangle^2 \right] = \min_{\{c_j\}_{j \in [k]}} \sum_{i=1}^n \min_{\alpha, j} (x - \alpha c_j)^\top \mathbf{E}[qq^\top] (x - \alpha c_j)$$

$$\begin{aligned}
&= \min_{\{c_j\}_{j \in [k]}} \sum_{i=1}^n \min_{\alpha, j} \|(x - \alpha c_j)\|_2^2 \\
&= \min_{\{c_j\}_{j \in [k]}} \sum_{i=1}^n \min_j \left\| x - \frac{\langle x, c_j \rangle}{\|c_j\|_2^2} c_j \right\|_2^2.
\end{aligned}$$

The second-to-last equality follows from the isotropy of \mathcal{Q} and the last equality follows from the fact that $\frac{\langle x, c_j \rangle}{\|c_j\|_2^2} c_j$ is the projection of x onto c_j . \square

B Quantized Projective k -Clustering

B.1 Proof of Fact 2.3

$$\begin{aligned}
\min_{\{\bar{u}_j\}_{j \in [k]}} \sum_{j=1}^k \left\| X_j - \bar{u}_j v_j^\top \right\|_F^2 &= \min \sum_{j=1}^k \left\| (X_j - \sigma_j u_j v_j^\top) + (\sigma_j u_j v_j^\top - \bar{u}_j v_j^\top) \right\|_F^2 \\
&\leq \min \sum_{j=1}^k \left\| X_j - \sigma_j u_j v_j^\top \right\|_F^2 + \left\| \sigma_j u_j v_j^\top - \bar{u}_j v_j^\top \right\|_F^2 \\
&= OPT + \min \sum_{j=1}^k \left\| \sigma_j u_j v_j^\top - \bar{u}_j v_j^\top \right\|_F^2 \\
&= OPT + \min \sum_{j=1}^k \left\| (\sigma_j u_j - \bar{u}_j) v_j^\top \right\|_F^2 = OPT + \min \sum_{j=1}^k \|\sigma_j u_j - \bar{u}_j\|_2^2
\end{aligned}$$

where the last line follows from the fact that v_j^\top is a one-dimensional rotation matrix.

C Anisotropic Loss

When all $x \in X$ have identical ℓ_2 -norm, it is sufficient to consider the ratio h_\perp/h_\parallel . We plot the value of h_\perp/h_\parallel for $t = 0.2$ in Figure 5 to illustrate how the loss function changes in terms of the norm of the input vector x .

As illustrated in the figure, as $\|x\|_2$ approaches t (from above) the ratio h_\perp/h_\parallel tends to 0 indicating that only the parallel component of the residual matters, i.e. just the projection of the center onto x is penalized. Although, when $\|x\|_2 \gg t$, the ratio h_\perp/h_\parallel approaches 1 resulting in weighting the parallel and residual components equally. This reduces the loss function to the loss function for k -means clustering: $\min_c \sum_{i=1}^n h(\|r_\parallel(x_i, c)\|_2^2 + \|r_\perp(x_i, c)\|_2^2) = \min_c \sum_{i=1}^n \|x_i - c\|_2^2$.

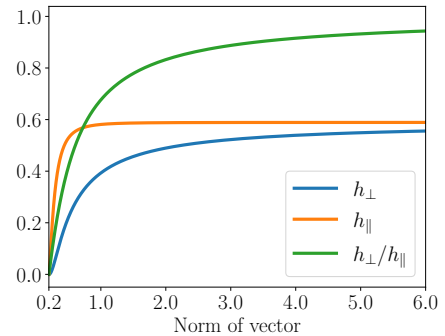


Figure 5: h_\parallel, h_\perp and h_\perp/h_\parallel for $t = 0.2$ and $d = 4$.